Ann. Rev. Astron. Astrophys. 1983. 21 : 209–37

HERBIG-HARO OBJECTS

Richard D. Schwartz

Department of Physics, University of Missouri, St. Louis, Missouri 63121

1. INTRODUCTION

The peculiar, semistellar emission nebulae called Herbig-Haro (HH) objects were discovered independently by Herbig (72, 73) and Haro (63, 64) in the course of Hα-emission star surveys of a dark-cloud region immediately south of the Orion Nebula. The prototype objects HH 1, 2, and 3, located near NGC 1999, each exhibit structure with tightly grouped knot-like condensations (see Figure 1). The spectra of HH objects are usually dominated by hydrogen Balmer emission lines and low-excitation emission lines of [O I], [S II], [N I], [Fe II], with moderate strength [O II] and [N II] lines, and relatively weak [O III] emission. Their locations in or near dark clouds in regions of star formation led to early speculation that the objects are associated with processes of star formation (2). Indeed, their properties and apparent lack of coincidence with visible young stars (e.g. T Tauri stars) led to the suggestion that the HH objects are themselves the sites of prestellar activity (75, 76). This notion still persists in some popular astronomy texts, although investigations over the past ten years have established that the HH objects are most likely the by-products of star formation rather than incipient stars.

Wide-ranging observations from the ultraviolet to the radio region of the spectrum have only recently illuminated the questions surrounding the origin and physical nature of the HH objects. This review summarizes the observational characteristics of these objects and presents the theoretical scenarios that have been advanced to account for their properties. Several reviews of HH objects have appeared within recent years. Cantó (30) has provided a broad overview of observations and theory with emphasis on radio observations. Böhm's (8–10, 12) reviews detail optical and infrared observations and theoretical models of HH objects. Dopita's (47) work is contained within a broader review of interstellar shock-wave phenomena, and in particular relates the optical and ultraviolet observations of HH

0066–4146/83/0915–0209$02.00

objects to shock-wave models. Other reviews have been given by Rodríguez (111) and Gyul'budagyan (60, 61). Most recently, a symposium on HH objects and T Tauri stars held in Mexico City (February 24–26, 1983) to honor Dr. G. Haro has added measurably to our present understanding of HH objects. The proceedings of the symposium, which may be considered as a major update to this review, are to be published in a special issue of *Revista Mexicana de Astronomía y Astrofísica* [Volume 7 (1983)].

2. THE NATURE OF HH NEBULAE: REFLECTION OR EMISSION?

The central enigma that persisted in the first 25 years of investigation of HH objects was the question of their source of excitation. In an early spectroscopic study, Böhm (7) set limits on the presence of a hot star in HH 1 based upon the character of its emission-line spectrum and the absence of a detectable star (64). Osterbrock (105) was the first to suggest that excitation might result from an energetic outflow of material from a young star. Magnan & Schatzman (97) proposed that energetic (100 MeV) protons plowing through a neutral medium could produce the required ionization state. A model in which ionizing transition radiation is produced by the encounter of 1 MeV electrons with dust grains was proposed by Gurzadyan (57, 58).

An important step toward the understanding of HH objects occurred with the observations of the Stroms and their co-workers (131, 132, 135) in which embedded infrared (IR) sources were discovered in the vicinities of several HH objects. In HH 24, broadband optical polarization measurements revealed relatively large polarization in two condensations, with electric vectors indicating a reflection origin from an IR source located amid, but not coincident with, the HH 24 condensations (132). A scenario was suggested wherein the HH objects are produced by circumstellar emission that penetrates through "tunnels" in the circumstellar dust shell of a young star, reflecting from dust condensations far removed from the star. However, this picture encountered difficulties in that other HH nebulae failed to exhibit significant polarization, and the nebular emission lines indicated an origin in a low-density medium ($n_e \lesssim 10^4$ cm^{-3}), which is not indicative of the densities of circumstellar gas interior to the dust shell of a young star. Gyul'budagyan (59) concluded that HH objects might be divided into two classes: those showing intrinsic emission and those showing pure reflection.

In the late nineteenth century, Burnham (25, 26) noted that the star T Tauri was embedded within a close-lying nebulosity. Herbig (71) later detected [O II] and [S II] emission extending to 8″ south of the star, and a

more detailed spectrum obtained by Schwartz (118, 119) revealed that Burnham's nebula was very similar to the prototype HH nebulae. Moreover, an additional HH nebula was discovered on the starward rim of Hind's reflection nebula (NGC 1555) about 30″ west of T Tauri (119). Whereas Hind's nebula exhibits only strong red continuum and Hα emission indicative of reflection from the star, the HH nebula appeared as a distinct emission nebula with strong, low-excitation emission lines. Its relatively high negative radial velocity (-60 km s^{-1}) contrasted with the positive velocity ($+37$ km s^{-1}) of the Hα line in reflection from dust in Hind's nebula in apparent movement away from the star.

The similarity of the spectra between the HH nebulae and the quasi-stationary knots in supernova remnants led Schwartz (119) to suggest that the classical HH objects are the result of the interaction of a supersonic stellar mass outflow with ambient gas, creating radiative shocks. It was further suggested that some HH objects (notably HH 24, which shows a stronger red continuum than most HH nebulae) possess a continuum component caused by reflection from dust, as in the scenario of Strom et al. (135). However, the nebular emission lines were predicted to arise in situ by shocked gas and hence to lack polarization. This expectation was borne out by the spectropolarimetric observations of HH 24 by Schmidt & Miller (116) and similar work on HH 30 by Cohen & Schmidt (38). Thus, the emission-line spectra of "classical" HH nebulae appear to arise as a result of mass outflow from a young star, and in some instances a continuum reflection component from the star is visible, contiguous with the emission nebula.

3. OBSERVATIONAL FACETS

3.1 *Optical Studies*

3.1.1 SURVEYS Following the early lists of HH objects (63–65, 72, 73). Herbig (78) compiled a photographic catalog containing information on 42 objects located mainly in the NGC 1333 complex, the Taurus-Auriga dark clouds, and the Orion complex. An objective prism Schmidt survey of selected southern dark clouds by Schwartz (121, 122) yielded 14 additional objects situated mainly in T-associations in Chamaeleon, Lupus, and Norma. This survey also uncovered the unusual objects HH 46/47, which are associated with a small dark globule located in the Gum Nebula (121). Additional HH objects with spectroscopic identifications have been reported by Strom et al. (135), Münch (99), Elias (51), Adams et al. (1), Cantó et al. (31), Cohen (35), and Gull et al. (56). Gyulbudaghian et al. (62) identified 37 possible HH objects in the Palomar atlas on a morphological basis. However, Cohen (35) has found that only a small fraction of these

"GGD" objects exhibit the emission-line spectra characteristic of HH nebulae. A similar morphological survey in southern dark clouds has been conducted by Reipurth (110), who reported 16 candidate objects. In total, less than 100 HH objects have been identified spectroscopically. However, since all surveys have been somewhat limited in areal coverage with differing limiting magnitudes, it is probably safe to surmise that many additional objects exist, especially at faint ($m > 19$) limits.

3.1.2 SPECTROSCOPIC STUDIES The early spectroscopic investigations of HH 1 by Böhm (7), Osterbrock (105), and Haro & Minkowski (66) firmly established the peculiar nature of the object in comparison with photoionized nebulae. The image tube photographic spectrum of HH 1 reported by Böhm et al. (17) revealed a plethora of low-excitation lines rarely seen in photoionized nebulae, including lines of [Fe II], Ca II, [N I], and Mg I]. Diagnostic plots of n_e vs T_e suggested average physical conditions typical of emission nebulae ($T_e \sim 10^4$ K, $n_e \sim 10^4$ cm^{-3}). However, electron densities obtained from the red [S II] doublet were found to be about four times higher than indicated by the [O II] doublet, presaging later shock-wave interpretations. Photographic spectra of 14 HH objects were published by Strom et al. (135), and Schwartz's spectra of the T Tauri nebula revealed its similarity to HH spectra and its dynamic connection to the star (119).

Well-calibrated spectrophotometric measurements began with the work of Böhm et al. (18, 19) on HH 1 and 2. A faint blue continuum increasing toward shorter wavelengths was seen (18), and reliable reddening corrections were derived using observations of the violet and infrared [S II] lines that arise from common upper-energy states (19). This work was continued with an elemental abundance analysis in HH 1 (15), which revealed essentially solar values. Brugel et al. (22, 23) extended the spectrophotometric work to 12 northern HH objects, and Böhm et al. (16) reported upon the very-low-excitation character of HH 7 and 11.

Spectrophotometry of separate portions of HH 1 indicated a large gradient in excitation (120), supporting the shock-wave interpretation. Dopita (44) measured the HH 46/47 system, discovering that HH 47 is of extremely low excitation with a high negative radial velocity (-140 km s^{-1}). Dopita's spectrophotometric work was extended to 18 objects, and the spectra were interpreted within the framework of theoretical shock-wave models (45). Raymond (108) had earlier explored shock-wave model fits to the emission-line intensities in HH 1.

Schwartz & Dopita (125) combined spectrophotometric and radial velocity data on 6 southern HH objects with similar data on 20 northern objects to explore the relation of excitation state to the nebular dynamics. A strong correlation was found in that the highest velocity objects tend to

exhibit the lowest excitation spectra, suggesting that the mass flow responsible for the shocks interacts with material that has already achieved a substantial velocity away from the star. The moderate- and high-dispersion spectra of HH 1 obtained by Schwartz (123, 124) revealed differential radial velocities between high- and low-excitation emission lines, a feature consistent with postshock gas flow. Moreover, the higher excitation lines of [O III] were found to possess a greater width than the low-excitation lines of [O I] and [N I], indicating greater macroturbulence or flow divergence in the hot portion of the shock than in the recombination zone.

The faint blue-UV continuum discovered by Böhm et al. (18) has been the target of more recent work. Brugel et al. (22) found $F_\lambda \propto \lambda^{-n}$, with $2.0 \lesssim n \lesssim 2.9$ for six objects. Dopita (47) noted that such a spectral index could be achieved by the combination of a Paschen continuum with an enhanced nebular two-photon (2q) continuum from hydrogen and helium. Moderate-resolution spectrophotometry of the continuum in 11 HH objects by Dopita et al. (48) revealed a striking correlation in that the lowest excitation objects exhibit the highest relative contributions of blue-UV continua. The interpretation of the HH continua is considered in more detail in Section 3.3.

Emission-line intensities for a relatively high-excitation object (HH 2H) and a low-excitation object (HH 47) are reproduced in Table 1 from the work of Dopita et al. (48). Raw and reddening-corrected intensities relative to $F(\mathrm{H}\beta) = 100$ demonstrate the range of excitation found in such objects. Note particularly the absence of [O III] in HH 47 and its intense lines of [N I] λ5200; [O I] λ6300, 6363; and [S II] λ6717, 6731 in comparison with the same lines in HH 2H. Also, the Balmer decrement remains relatively steep in HH 47 after correction for reddening, a signature of the importance of collisional excitation, which dominates in low-velocity shocks.

Cantó (30) has compiled radial-velocity information on about 45 HH objects, demonstrating that about 75% of the objects exhibit negative radial velocities. At least 5 objects are known with $V \lesssim -150$ km s^{-1}, with only two objects possessing $V > +80$ km s^{-1}. The conventional interpretation is that the HH objects are ejected from young stars embedded within dark clouds, and that a selection effect is imposed in that we tend to see those objects ejected into the foreground of the clouds, but not those objects ejected away from us (which usually remain deep within or behind the dark cloud).

3.1.3 PROPER MOTIONS AND ALIGNMENTS The large radial velocities observed in a number of HH objects indicated that some might be expected to exhibit large tangential velocities. Luyten (95a, 95b) first detected large

Table 1 Representative spectra of high- and low-excitation HH objects

Line identification	λ(Å)	HH 2H		HH 47	
		F^a	$F_0{}^b$	F^a	$F_0{}^c$
[O II]	3727, 29	148.2	222	81.3	87.1
H 10	3797	2.9	4.3	—	—
H 9	3835	4.6	6.6	—	—
H 8, He I, [Ne III]	3868	16.7	23.7	—	—
Hε, He I	3889	11.5	16.2	7.4	7.8
Ca II	3934	12.6	17.7	44.1	46.6
Ca II, [Ne III]	3968	25.7	35.1	48.5	51.1
[S II]	4068, 76	53.1	70.0	77.3	81.0
Hδ	4101	19.9	25.9	19.5	20.4
[Fe II]	4245	5.9	7.3	15.1	15.6
[Fe II]	4276, 87	6.9	8.4	26.6	27.5
Hγ	4340	38.3	45.8	42.4	43.7
[O III], [Fe II]	4363	12.4	14.7	5.2	5.3
[Fe II]	4415	7.2	8.4	16.7	17.1
[Fe II], Mg I]	4562, 71	3.7	4.1	38.3	39.0
He II	4686	8.0	8.5	—	—
Hβ	4861	100		100	
[O III]	4959	30.2	29.3	—	—
[O III]	5007	85.0	81.4	<1.0	<1.0
[Fe II]	5158	21.3	19.4	38.6	39.2
[N I]	5198, 200	11.8	10.6	129.3	127.0
[Fe II]	5261, 73	17.8	15.7	20.3	19.9
[Fe II]	5334	4.7	4.0	4.0	3.9
[Fe II]	5528	4.9	4.0	—	—
[N II]	5755	8.8	6.8	—	—
He I	5876	8.8	6.6	—	—
[O I]	6300	202	138	342	320
[O I]	6363	75.3	50.1	108.6	101.4
[N II]	6548	74	47.4	27.7	25.7
Hα	6563	538	342.7	500	463.2
[N II]	6583	287	182.1	72.5	67.1
He I	6678	2.5	1.6	—	—
[S II]	6717	70.2	43.3	486.2	488
[S II]	6731	138.2	85.1	511	471
[Fe II]	7155	51.7	29.6	32	29
[Fe II]	7172	10.0	5.7	14	12.7
[Ca II]	7291	50.3	28.2	125	113
[O II], [Ca II]	7318, 24, 30	173	96.3	71	64
[Fe II], [Ni II]	7376	25	13.8	32	29

[a] Observed relative intensities.
[b] Corrected for reddening with $C(H\beta) = 0.59$.
[c] Corrected for reddening with $C(H\beta) = 0.10$ [see Dopita et al. (48) for details of reddening determinations].

proper motions in HH 28 and 29, two objects associated with the L 1551 dark-cloud complex in Taurus. Cudworth & Herbig (42) measured these objects and found that both proper motion vectors were directed away from the vicinity of an embedded IR source discovered by Strom et al. (134), which was suggested to be the exciting source of an adjacent extended nebulosity designated HH 102. The large tangential velocities ($\sim$200 km s^{-1}) of HH 28 and 29 and their relatively great distances (2.8′ and 8′ corresponding to 0.12 pc and 0.35 pc, respectively) from the exciting star indicate that energetic flows or ejection episodes are associated with the exciting star. Supporting evidence for this from radio observations of the L 1551 region is discussed in Section 3.4.2.

Large proper motions for HH 1 and 2 were discovered by Herbig & Jones (80). In this case, HH 1 and 2 were found to be moving in opposite directions from a 17th mag T Tauri star located between the two objects. Cohen & Schwartz (39) had earlier discovered that the star (C-S star) is a relatively strong IR source, suggesting that it might be the exciting star for HH 1 and 2. Figure 2 represents the proper motion vectors in HH 1 and 2 as measured by Herbig & Jones. The large tangential velocities (up to 350 km s^{-1}) implied by the proper motions and the shock velocities ($\lesssim$100 km s^{-1}) required to produce the optical spectra indicate that the shocks are being produced against material that already possesses substantial outward motion from the star. The alignment of the HH nebulae with the star evident in Figures 1 and 2 is suggestive of a highly anisotropic (bipolar?) flow from the star.

A third case of high proper motions has been discovered by Jones & Herbig (83) in the knots of HH 39, which lie on the axis of symmetry of Hubble's nebula (NGC 2261), a nebula associated with the young variable R Mon. The objects appear to be in motion away from R Mon and the fan-shaped nebula. Radio measurements of CO by Cantó et al. (33) (see Section 3.4 below) in the NGC 2261 region suggest the presence of bipolar gas motions, the visible fan nebula corresponding with the direction of one of the CO lobes. In a fourth case, a southeastward proper motion vector for HH 43 found by B. Jones (private communication) was used by Cohen & Schwartz (41) in an IR search to locate the probable exciting star. The IR source, HH 43, and HH 38 are situated along a straight line.

A number of other HH systems exhibit alignments suggestive of directed, bipolar motion. The objects HH 7–11 form a chain of nearly equally spaced condensations that fall on a line passing through a strong infrared source. A high-resolution photograph of HH 24 by P. Wehinger (private communication) reveals that one of the elongated condensations actually consists of a string of 5 closely spaced knots aligned with the IR source. One of the most remarkable examples is the HH 46/47 system in which Dopita et al.

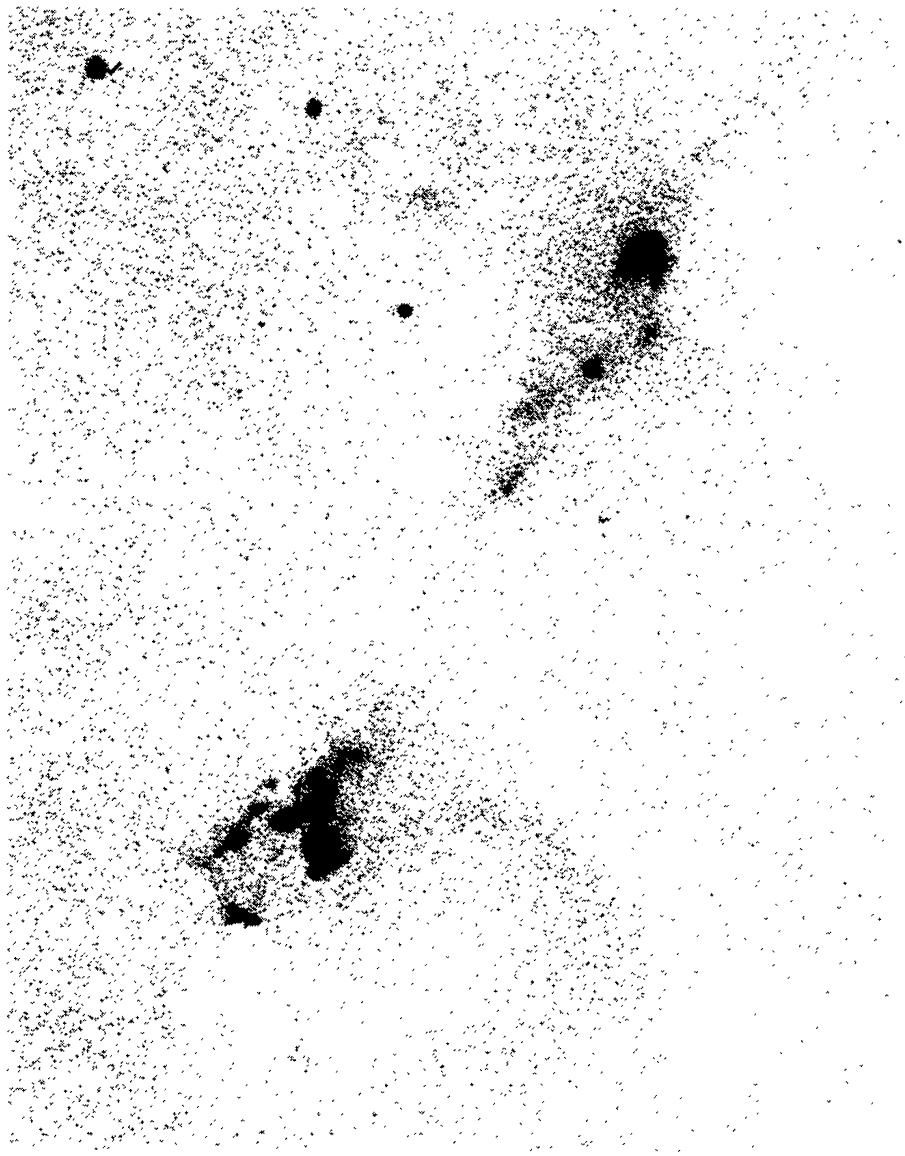

Figure 1 The prototype HH objects: HH 1 and 2. See Figure 2 for identifications and scale [from Herbig & Jones (80) and kindly supplied by the authors].

(49) have found HH 47 to be ejected from a source in a small dark cloud. While HH 47 has been ejected outside the cloud boundary with a radial velocity component of -140 km s^{-1}, a "counter" HH object (HH 47C) has been found to have emerged from behind the cloud with a velocity of $+100$ km s^{-1}. The objects lie on a straight line with an embedded T Tauri star located midway between the objects as shown in Figure 3. Another linear alignment of HH nebulae has recently been reported by Mundt et al. (101) for the HH 32 system around the T Tauri star AS 353A.

3.1.4 VARIABILITY Although optical variations were noted early in the study of HH objects (74), it was the photographic photometry of the knots

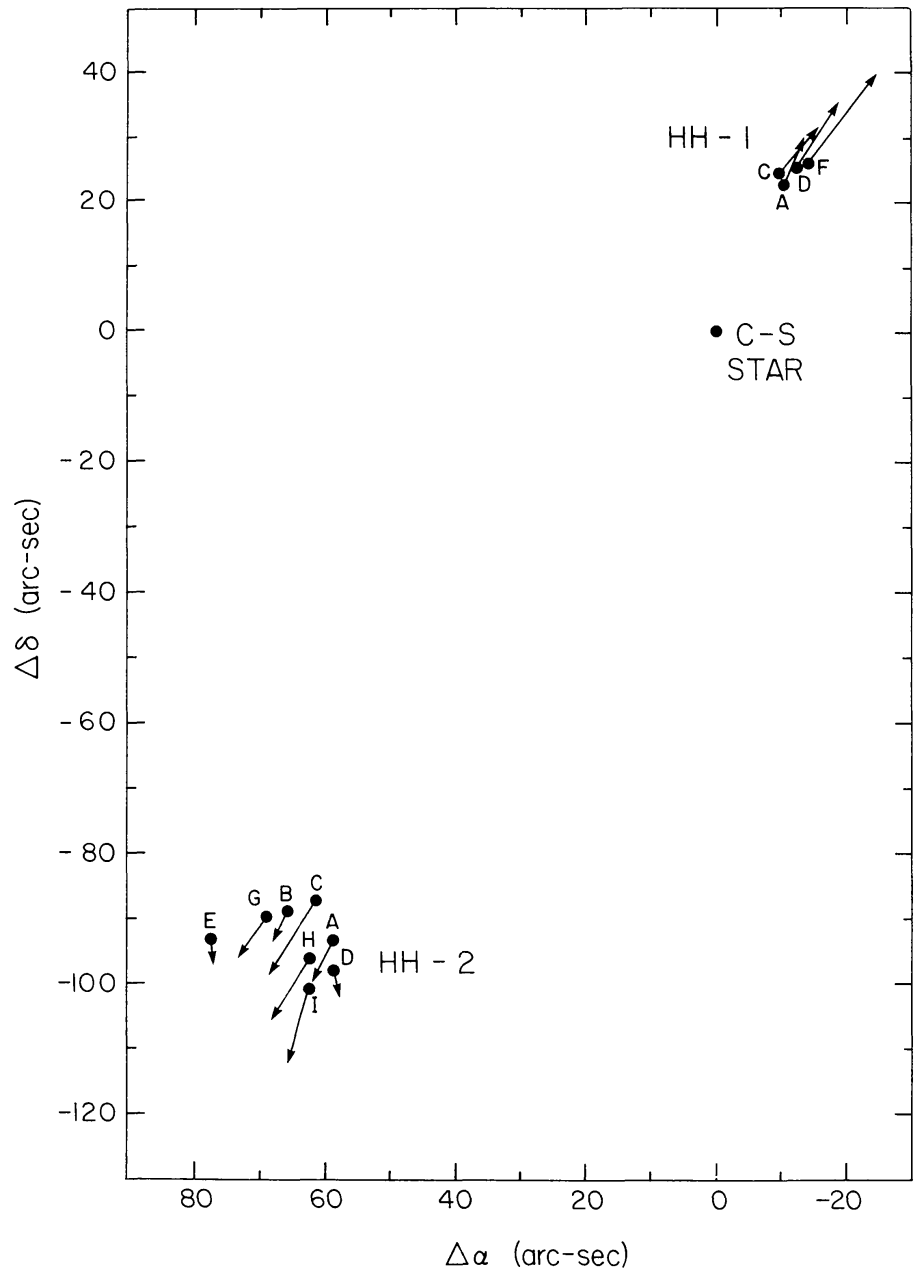

Figure 2 The proper motion vectors indicating 100-year motions for the individual knots in HH 1 and 2. The C-S star is a 17th mag T Tauri star that has evidently ejected the HH objects [from Herbig & Jones (80)].

in HH 1 and 2 by Herbig (75, 77) that established the general character of the light changes. HH 2H and 2G were observed to increase gradually in luminosity by approximately a factor of 6 between 1950 and 1955, with a slow additional *increase* of about a factor of 2 by 1973. During the same interval, HH 2 A,B appeared to *decrease* by about a factor of 4. Schwartz (123) pointed out that the timescale of the variations is comparable to the excitation or recombination timescales expected from the onset or

termination of shock-wave excitation. It was noted that knots HH 2A and 2B lie to the NW of HH 2H and 2G (see Figures 1 and 2), and that the variation sequence might be related to the propagation of an impulse from the NW to the SE. Similarly, HH1 was noted to brighten sequentially from

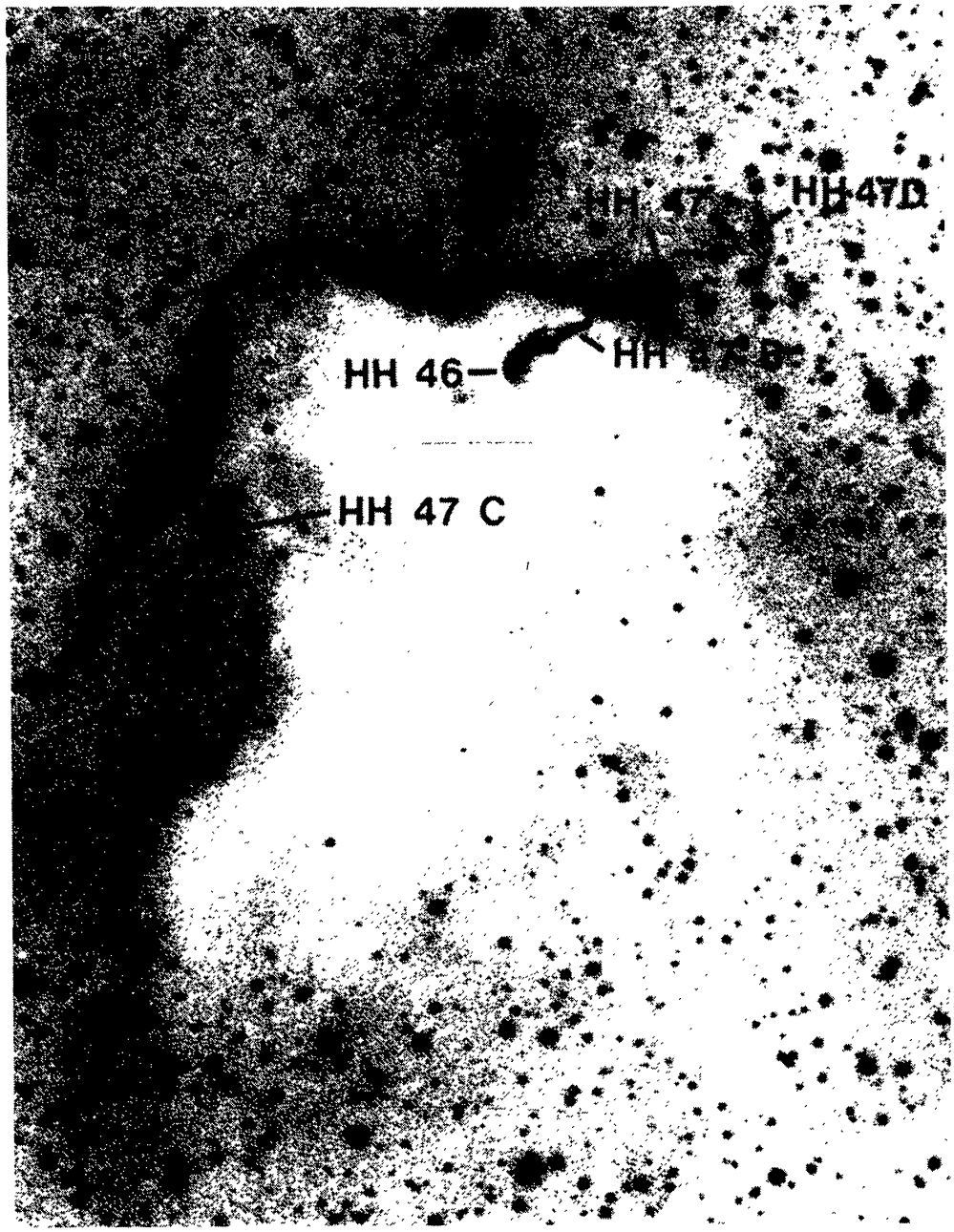

Figure 3 The HH 46/47 system [see Dopita et al. (49)]. North is up, east to the right. HH 46 is a combined emission/reflection nebula, reflecting light from a T Tauri star embedded immediately to its SW. A bridge of emission (47B) attaches HH 46 to HH 47. HH 46, 47B, and 47 exhibit high negative radial velocities indicating ejection through the front side of the cloud, whereas 47C can be seen emerging behind the cloud with a high positive velocity (photograph kindly provided by Bart Bok).

the SE to the NW portion of the object. In both cases, the variations appear to be consistent with the propagation of disturbances from the C-S star.

Böhm (10) has discussed both the luminosity and spectral variations observed in HH1 and 2 (15, 17, 19), suggesting that changes in n_e or T_e by a factor of $\lesssim 2$ could produce the variations. Again, this was interpreted within the framework of a time-dependent shock—in this case, of a spherical shock propagating outward from the center of an HH condensation (11), which was presumed to contain an internal, variable source of excitation.

3.1.5 POLARIZATION As discussed in Section 2, broadband measurements of knots in HH 24 yielded high polarizations ($\sim 20\%$), with electric vectors indicating a reflection origin from an embedded IR source (132). The spectropolarimetry of these knots by Schmidt & Miller (116) revealed that the nebular emission lines were unpolarized, but that the continuum possessed large polarization ($\sim 30\%$) characteristic of reflection. Moreover, the Hα-emission line exhibited a small but significant polarization, suggesting a combination of unpolarized nebular emission and reflection from an embedded Hα-emission star.

Broadband polarization measurements of other HH objects were reported by Strom et al. (132), Schmidt & Vrba (117), King & Scarrott (85), and Vrba et al. (139). In general, polarization is found to be lacking above that expected from an interstellar component. However, significant polarization was reported for HH 100 in the Corona Austrina complex (139). A spectrum of this object taken by Schwartz (unpublished) reveals a relatively strong red-continuum component, as in HH 24; thus HH 100 likely represents another case of combined emission and reflection.

Spectropolarimetry of HH 30 by Cohen & Schmidt (38) revealed a faint polarized continuum, with an electric vector indicating a reflection origin from the nearby T Tauri star HL Tau (which itself is wrapped in an HH nebula like T Tauri). The nebular emission lines in HH 30 were found to be unpolarized. It should be emphasized that the polarization, when present, appears to be associated with a predominantly red-continuum component, such as what one would expect in reflection from a T Tauri star. The blue-UV continuum, which is probably present in most if not all HH objects, may be largely of nebular origin (see discussion in Section 3.3) and thus unpolarized, although this speculation has yet to be borne out by careful spectropolarimetric measurements.

3.2 *Infrared Studies*

3.2.1 GROUND-BASED OBSERVATIONS The first association of an embedded IR source with an HH object occurred in the study of HH 100 (135, 136) in the Corona Australis complex by Strom et al. (131). The IR source,

estimated to suffer a visual extinction of 15 mag, was found to possess a 1.2–10 μm energy distribution similar to that of other Orion population stars, and a luminosity $L_{IR} \gtrsim 13\ L_{\odot}$. A subsequent survey by Strom et al. (135) revealed IR sources in the vicinities of HH 12, HH 7–11, and HH 24 (M 78 HH). Photometry of the HH 12 source demonstrated its similarity in IR energy distribution to those of HL Tau and T Tau. The Stroms and Vrba (133, 134, 137, 138, 140) identified large numbers of IR sources in dark-cloud regions, a few of which have proved to be associated with HH objects (e.g. the L 1551 IRS 5 source for HH 28 and 29, and a new IR source in NGC 1333 near the NW end of the chain of objects HH 7–11).

In a study of the Taurus dark-cloud complex, Elias (51) found that the HH object Haro 6–10 (65) is coincident with a strong variable IR source, again with IR colors reminiscent of a heavily obscured T Tauri star. Systematic mapping of 2 arcmin square regions at 2.3 μm centered on HH objects was carried out by Cohen & Schwartz (39, 40). Several interesting IR sources were discovered, including the C-S star between HH 1 and 2, and the source near HH 7–11. Positional measurements on the HH 7–11 source placed it about 15 arcsec north of the position reported by Strom et al. (137), thus putting it about 15 arcsec NW of HH 11 and on a line passing through the HH 7–11 chain. In addition, K-L colors of these objects were indicative of those expected from embedded T Tauri stars. These first searches were hampered by the lack of any discriminating criteria that could narrow the search limits. To detect sources more than 1 arcmin from an HH nebula and with a limiting magnitude of $K \lesssim 11.4$ required lengthy search times.

With the recognition that the exciting stars are often aligned with HH nebulae when two or more nebulae appear close together (e.g. HH 7–11), and with proper motion information indicating the direction of the exciting source in several cases, Cohen & Schwartz (41) were able to narrow the IR search fields. Concentrating IR scans in the directions suggested by alignments and proper motions, 10 new IR sources were identified as probable exciting stars for HH objects. Astrometry and 1.6–20 μm photometry on each of 16 HH IR sources were reported. On the basis of the near-IR photometry and extrapolated fluxes beyond 20 μm, lower limits on the bolometric luminosities were found for the sources. A wide range of luminosities is indicated, from 0.7 $L_{\odot}$ for the HH 31 source to 850 $L_{\odot}$ for R Mon (the HH 39 source). Most of the sources fall between 1 $L_{\odot}$ and 30 $L_{\odot}$, typical of values expected from T Tauri stars. Moorwood & Salinari (98) have independently discovered the HH 7–11 IR source in NGC 1333, reporting a position, color, and luminosity consistent with the work of Cohen & Schwartz (40, 41). Beichman & Harris (6) have reported IR photometry of L 1551 IRS 5, suggesting that its present luminosity ($\sim 30\ L_{\odot}$) is insufficient to support a steady flow of the magnitude discovered in CO measurements by Snell et al. (130, see Section 3.4). It is suggested that

the source has undergone a FU Ori-type outburst at some time in the past, resulting in an impulsive mass flow that produced both HH 28 and 29 and the molecular flow.

Silicate absorption features near 10 μm have been seen in 4 of the sources studied by Cohen & Schwartz (41), and in the HH 100 IR source by Whittet et al. (141). Also, 3.1-μm ice absorption has been seen in HL Tau (36, 114a), the exciting star of a close-lying HH nebula, and in the HH 100 IR source (141).

Infrared spectrophotometry of the HH nebulae has revealed the presence of H_2 emission in a number of objects. Beckwith et al. (5) detected emission from the near vicinity of T Tauri in the $v = 1 \rightarrow 0$ $S(1)$ line of H_2 at 2.12 μm. In an extensive survey, Elias (52) discovered H_2 emission from HH 1, 2, 24, 40, 46, 48, 53, and 54. Independently, Fischer et al. (53) detected extended H_2 emission in HH 2. Elias found that the line ratios in the $v = 1 \rightarrow 0$ $S(0)$ and $S(1)$ lines, and the $v = 1 \rightarrow 0$ $S(2)$ and $v = 2 \rightarrow 1$ $S(1)$ lines, were consistent with shock-wave heating of molecular gas at a density of 10^4 cm^{-3}, with a shock velocity of about 15 km s^{-1} (52). It should be emphasized that this is molecular gas associated with the HH nebulae sites, not with the (usually) displaced continuum IR sources assumed to represent the exciting stars. The H_2 line intensities appear to exclude any model of UV radiative excitation with lines formed by cascade, thus lending additional support to the shock-wave interpretation of HH nebulae. Most recently, Simon & Joyce (127) have reported H_2 emission from HH 7–10 and HH 12.

3.2.2 FAR-INFRARED OBSERVATIONS Fridlund et al. (54) reported the first detection of an HH IR source at far-IR wavelengths. Balloon-borne measurements of the L 1551 IRS 5 source at 85 μm and 150 μm, in combination with the earlier mid-IR measurements, led to a luminosity estimate of about 25 $L_\odot$. Harvey et al. (67, 68) used the Kuiper Airborne Observatory (KAO) to map HH objects at 50 and 100 μm. Sources were detected at the sites of HH 7–11 IRS, HH 1–2, HH 24, and L 1551 IRS 5. The far-IR positions in general coincide with the ground-based position measurements for the sources, although the far-IR sources are extended on a scale of 0.5–2 arcmin, with luminosities $L \sim 10^{2 \pm 0.5}$ $L_\odot$. Most recent KAO observations by Cohen, Harvey, Wilking & Schwartz (unpublished) have resulted in the far-IR detection of 7 of 9 sources reported by Cohen & Schwartz (41). In several cases, the extended structure is suggestive of that expected from the existence of a circumstellar disk and/or bipolar flows associated with dust.

3.3 *Ultraviolet Studies*

Even the brightest HH objects are quite faint ($R \sim 15$, dominated by lines of Hα and [S II]) and require large optical telescopes for detailed spectro-

scopic study. Moreover, their low-excitation character suggests that few satellite UV lines would be expected, and their locations in dark clouds imply the possibility of substantial extinction, further hindering potential UV studies. With these considerations, the detection of both UV continuum and emission lines in HH 1 by Ortolani & D'Odorico (104) with the IUE ranks as one of the more remarkable observational developments of recent years. In that study, emission lines of C II, C III], N III], and C IV were detected, signaling the presence of a high-temperature nebular component not clearly evident from the optical spectra. Moreover, after correction for extinction, a continuum rapidly increasing with decreasing wavelength was observed in the range $1200 \lesssim \lambda \lesssim 1900$ Å, suggesting the possible presence of a compact, very hot star.

Böhm et al. (13) also obtained short-wavelength UV spectra of HH 1 with the IUE, and extended observations to the range $1900 \lesssim \lambda \lesssim 3000$ Å. Fifteen emission lines were identified, including the four discovered by Ortolani & D'Odorico. Averaging the continuum over 100-Å bins, a very steep flux increase ($F_\lambda \propto \lambda^{-6.9}$) was observed from 3000 Å to 2400 Å, with a more gentle increase to 1200 Å. It was concluded that the spectrum could not be produced by light scattering from even an extreme T Tauri star, assuming reasonable dust-scattering properties. Combining the UV and optical data (22), Böhm et al. (13) concluded that if the continuum is caused by scattering of starlight the star must be very hot and close to the HH object. Böhm-Vitense et al. (20) extended the IUE observations to HH 2H, with results quite similar to those found in HH 1. Böhm & Böhm-Vitense (14) also observed the C-S star between HH 1 and 2, finding extended UV emission to at least 11 arcsec from the star with a spectral index similar to HH 1.

Dopita (47) first suggested that the UV continuum might be the product of enhanced two-photon (2q) emission from hydrogen. Spectrophotometry of 10 HH objects in the range $3300 < \lambda < 7000$ Å by Dopita et al. (48) revealed that the lowest excitation objects possess the largest blue-UV continua. A model involving a simple combination of free-bound (Balmer and Paschen) continuum and 2q (hydrogen and helium) continuum enhanced by a factor f over that expected from a pure recombination spectrum was successful in matching the observed continua. The 2q enhancement factors ranged from $f = 2.8$ for HH 2A to $f = 13.3$ for HH 47, and allowed reasonable fits to the IUE data on HH 1 and 2H to a lower wavelength limit of about 1500 Å. Detailed shock-wave models were computed for low-velocity shocks propagating in a medium of low fractional ionization (48). In this case, the dominant coolant is Lyman-α, and the postshock gas maintains a relatively high neutral fraction. Hence, collisional excitation dominates, with only a minor contribution from recombination cascades. As a result, the "excess" population of the

hydrogen 2s level leads to the 2q enhancement and is correlated with the excitation class of the nebula, as is observed.

The most serious objection to the enhanced 2q hypothesis was the apparent continuing increase of the UV flux observed shortward of 1400 Å (13, 104). The 2q flux should peak in the vicinity of 1400–1500 Å and decrease rapidly to zero at 1216 Å. However, interpretation of the short-wavelength data was hindered by a low signal-to-noise ratio and by the possibility of unresolved emission lines. Brugel et al. (24) have obtained improved statistics on the UV continuum in HH 2H, and report evidence of a turnover in the spectrum in the vicinity of 1500 Å, supporting the 2q hypothesis. Schwartz (124a) has recently obtained 1200–1900 Å IUE spectra of the low-excitation objects HH 43 and HH 47. As predicted by the shock-wave models (48), the UV continuum is quite prominent in these objects, and there is an indication of a 2q turnover near 1500 Å. The low-excitation objects exhibit none of the higher excitation UV lines (e.g. C IV λ1549, C III] λ1909) seen in HH 1 and HH 2. However, surprisingly strong H_2 lines from P5 and R3 transitions in the $v' = 1$ to $v'' = 3$, 6, 7, and 8 Lyman bands are found. Figure 4 is an extinction-corrected short-wavelength spectrum of HH 43 demonstrating the continuum and lines. The H_2 transitions are excited by fluorescence from the red wing of the H Lyman α line, and were first observed in the spectra of sunspots (82) and later in an IUE spectrum of Burnham's nebula (the HH nebula associated with T Tauri) obtained by Brown et al. (21).

The coexistence of a relatively low-excitation optical spectrum with a higher excitation UV spectrum in objects like HH 1 and HH 2H is somewhat enigmatic. No single plane-parallel shock-wave model is capable of producing this result, nor is the superposition of high-temperature and low-temperature shocks, since the high-excitation optical [O III] lines, for example, will be much too strong if the two shock areas are equivalent. It is possible that nonplanar shocks may yield hot spots which, when added to a low-temperature shock of a much larger area, would yield the required composite spectra. In addition, the shocks may result from nonsteady flows with postshock temperature-density regimes quite different from steady-flow shocks. This latter speculation receives some support from the light variations observed by Herbig (75). Pravdo & Marshall (107) reported the detection of X-ray emission from the vicinity of HH 1, which could signal the presence of very hot gas. However, the C-S star was included in the X-ray aperture, and the star could be the source of the X-rays since similar emission has been detected from other T Tauri stars (55).

3.4 *Radio Studies*

Owing to the excellent review of radio observations given by Cantó (30), this section deals primarily with recent results.

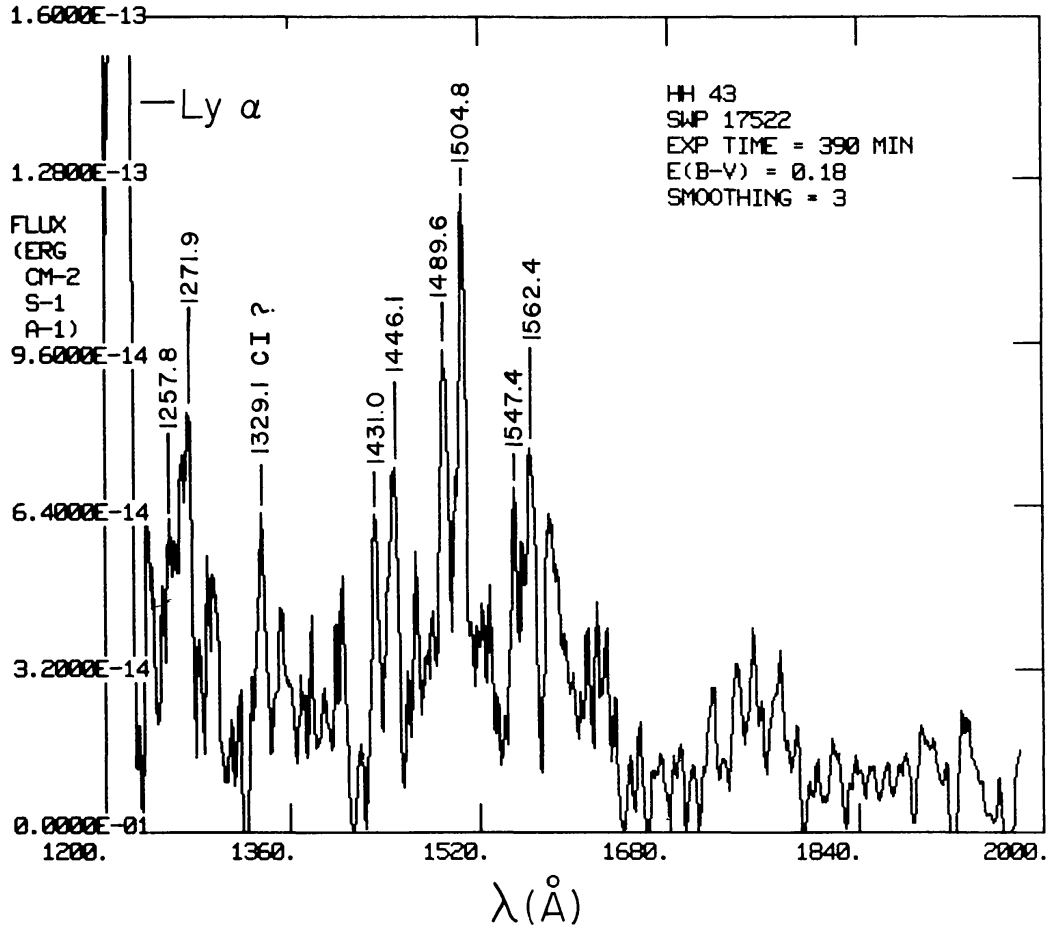

Figure 4 An ultraviolet spectrum of the low-excitation object HH 43, obtained by the author with the IUE. The most prominent lines arise from the Lyman band transitions of H_2, which are excited by fluorescence from Ly α. Eight of the H_2 lines from the R3 and P5 branches are identified by wavelength. A faint continuum appears to peak in the vicinity of 1500 Å. The Ly α line is due mainly to geocoronal emission [from Schwartz (124a)].

3.4.1 PROPERTIES OF MOLECULAR CLOUDS ASSOCIATED WITH HERBIG-HARO OBJECTS Millimeter-wave observations of molecular lines in the NGC 1333 (HH 7–11) and M 78 (HH 24) dark clouds were first reported by Lada et al. (90). Measurements of the lines of H_2CO, HCN, NH_3, CS, ^{12}CO, and ^{13}CO yielded a cloud temperature of about 20 K and an H_2 density of about 2×10^4 cm^{-3}. In each cloud, peak emission occurred in a broad ($\sim$1.5 pc diameter) plateau located in the vicinity of the HH objects and their suggested IR sources. In a study of the ^{12}CO and ^{13}CO lines in NGC 1333, Loren (94) found a velocity separation suggesting the presence of two clouds in collision, triggering star formation in the vicinity of HH 7–11. Later, Loren et al. (95) detected H_2CO emission from the regions of 12 of 30 HH objects, finding H_2 densities ranging from 10^4 to 9×10^4 cm^{-3} and temperatures from 9 K to 34 K. Peak densities were found to coincide spatially with IR source positions more than with the HH positions.

Ho & Barrett (81) found NH_3 emission from the near vicinities of 15 of 29 HH objects observed, and concluded that the dense [$n(H_2) > 5 \times 10^3$ cm^{-3}] neutral clouds found are not themselves the sites of ongoing star formation. The NGC 1333 and Serpens regions were mapped, with the results suggesting the presence of cloud fragmentation and rotation. MacDonald et al. (96) observed NH_3 and ^{12}CO linewidths in molecular clouds associated with the GGD objects, and found that turbulent or systematic velocities do not increase in the central cores of the clouds. Rodríguez et al. (114) studied the clouds associated with GGD objects using H_2O maser observations, NH_3 and CO observations, and continuum observations.

3.4.2 GAS FLOWS ASSOCIATED WITH HH IR STARS Perhaps the most important radio measurements bearing upon the origin of HH objects involve the detection of anisotropic mass flows associated with IR sources believed to be the exciting stars of HH objects. Although Knapp et al. (86) first detected a low-velocity wing in the ^{12}CO emission in the vicinity of HH 102 in the L 1551 dark cloud, it was the CO measurements of Snell et al. (130) that revealed broad velocity features, with redshifted CO in a lobe to the NE of L 1551 IRS 5 and blueshifted CO in a lobe to the SW of the IR source. Figure 5 displays the geometry of the CO emission relative to the IR source and HH 28 and 29. The HH objects have space motions (42) consistent with that expected from a directional flow in the SW CO lobe. Snell et al. proposed a model in which the star is obscured by a thick disk viewed nearly edge-on, with a strong stellar wind channeled into a bipolar flow as shown in Figure 6. A similar CO bipolar flow was discovered by Snell & Edwards (128) in the NGC 1333 complex centered upon the IR source aligned with HH 7–11. As shown in Figure 7, the HH objects appear to be associated with the blue-shifted CO lobe, and the overlapping redshifted and blueshifted lobes indicate that the flow has a significant radial component as compared with the L 1551 flow, which is mainly in the plane of the sky. Accordingly, the objects HH 7–11 also exhibit higher negative radial velocities than HH 28 and 29. Evidence for bipolar CO flow has also been reported by Snell & Edwards (129) for a source associated with HH 24 and for another source [see (41) for IR source location] near HH 25 and 26.

Additional evidence for anisotropic flows associated with HH objects was marshaled by Cantó et al. (33) in a study of R Mon, which is associated with Hubble's nebula (NGC 2261). A negative velocity CO lobe was found to be associated with the visible nebula, with a positive velocity CO lobe to the south of the star. Cantó et al. propose the presence of a disklike molecular cloud around R Mon, channeling a strong stellar wind into the

lobes. The northward collimated stream is interpreted as having glanced off another molecular cloud to the NW of NGC 2261, forming a focused shock wave at the location of HH 39. The proper motion studies of HH 39 by Jones & Herbig (83) further support the association of the HH object with a flow from R Mon. Other instances of apparent bipolar flows have been reported for GGD 12-5 and GGD 27-28 by Rodríguez et al. (112).

The realization that HH objects are associated with T Tauri stars led to CO velocity measurements toward such stars. Edwards & Snell (50) found high-velocity flows associated with T Tau, AS 353A, and HL Tau out of 28 T Tauri stars mapped. Interestingly, each of the three stars detected possess

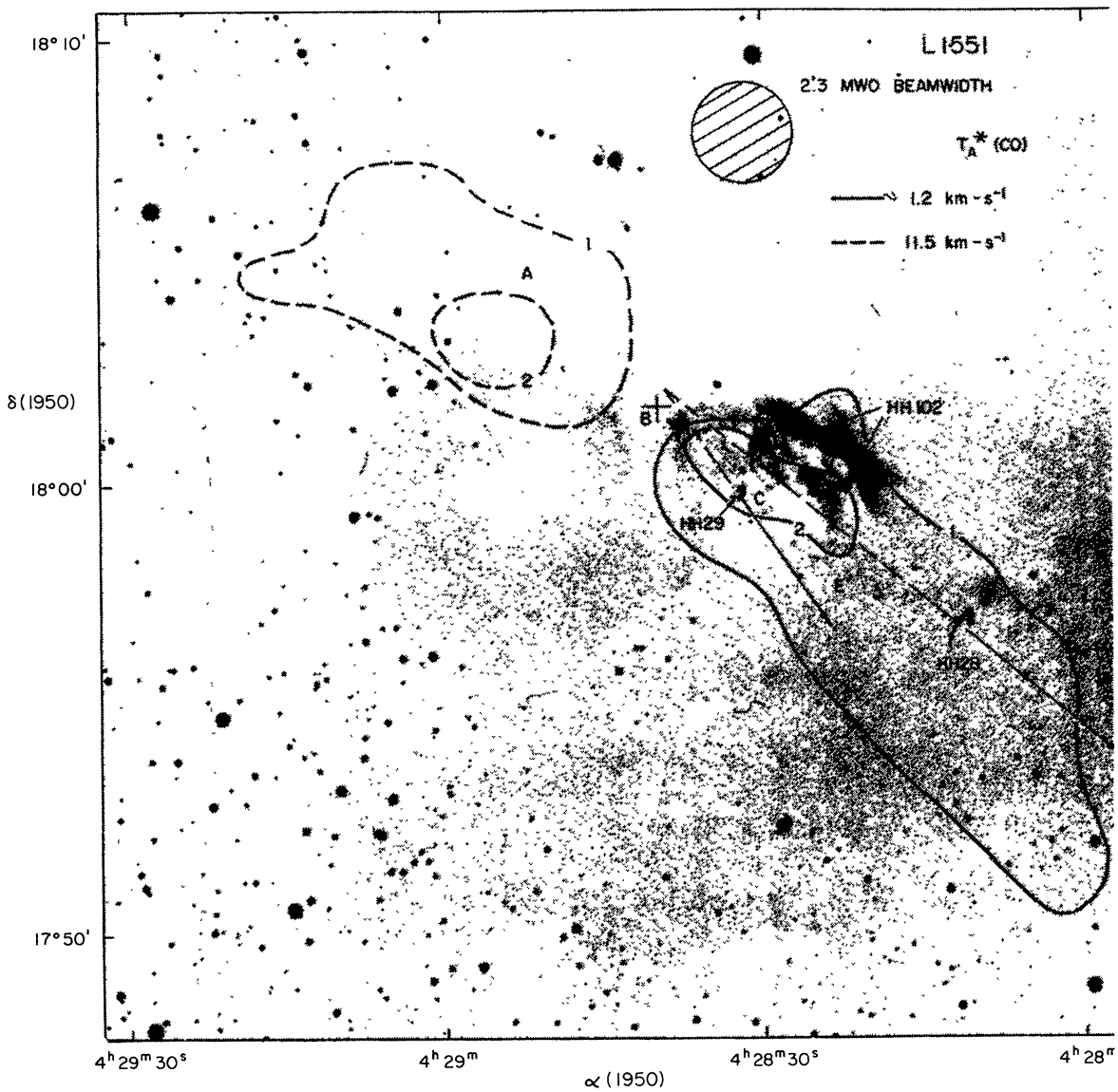

Figure 5 The bipolar CO flow associated with the source L 1551 IRS 5 (labeled *B* in the figure). HH 28 and 29 fall in the blueshifted lobe, with proper motions (42) indicating *B* as a source [kindly supplied by Snell et al. (130)].

nearby HH objects. Calvet et al. (27) independently discovered the flows in T Tau and HL Tau in a CO study of 12 T Tauri stars. Kutner et al. (89) have also reported the presence of broad CO line wings near T Tauri stars. Bally & Lada (3) have reported extensive measurements of high-velocity flows near young stellar objects, including some T Tauri stars and HH IR sources.

3.4.3 MASER EMISSION Maser emission in the 22-GHz line of H_2O was first detected by Dickinson et al. (43) from a source near the HH 7–11 group. Lo et al (92) independently detected this source along with another source in the direction of HH 1. Lo et al. (93) discovered short timescale variations in the HH 7–11 source with multiple-velocity components in the range -33 to 8 km s^{-1}, all blueshifted with respect to the molecular cloud. Haschick et al. (69) continued to monitor variations in this source, and they determined

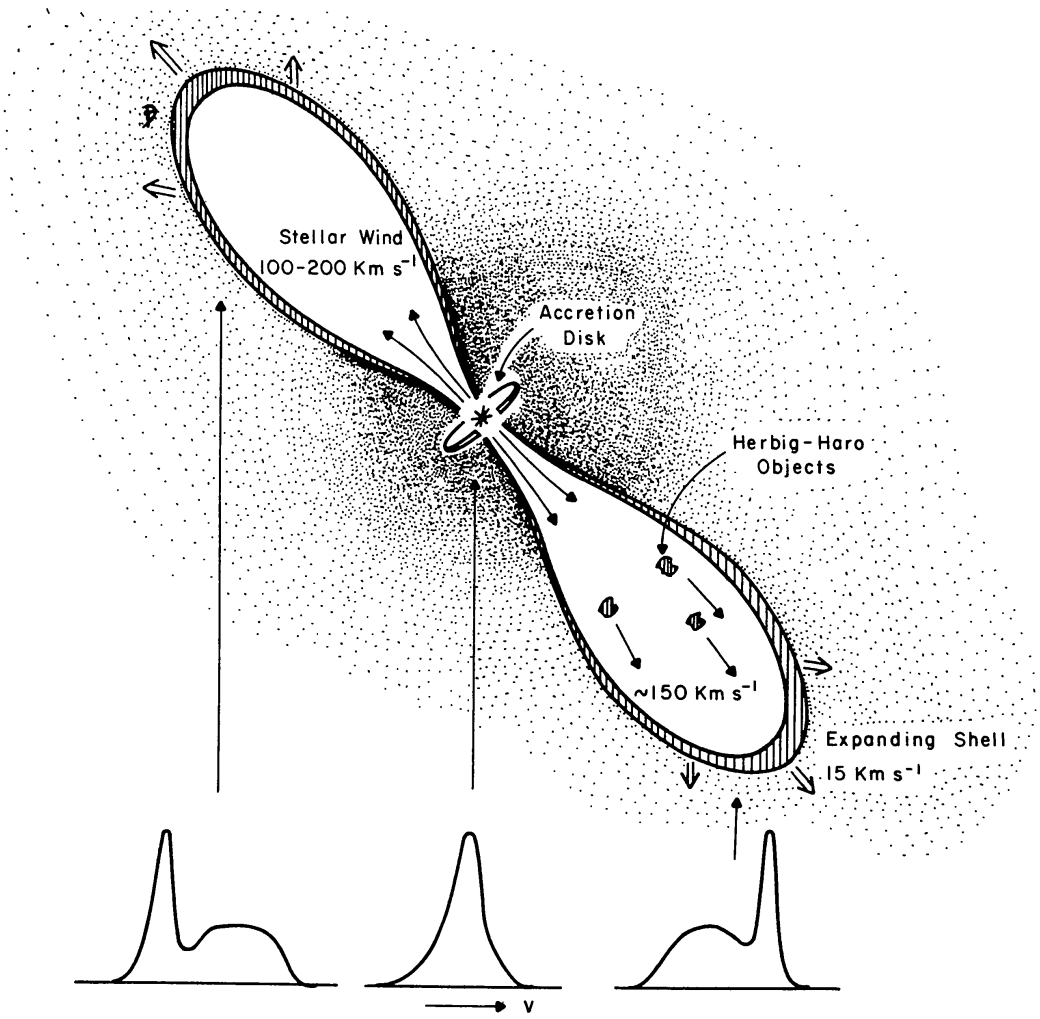

Figure 6 The model proposed by Snell et al. (130) to explain the L 1551 observations. The accretion disk visibly obscures the star, and the CO flow is driven by a stellar wind in which the HH objects are embedded.

an accurate interferometric position that placed it coincident with the position of the HH 7–11 IR source as measured by Cohen & Schwartz (40). Earlier, Knapp & Morris (87) had detected H_2O maser emission from a region about 0.9 arcmin NE of T Tauri. Most recently, Haschick et al. (70) detected H_2O emission from a region about 5 arcmin NE of HH 22/23. Rodríguez et al. (113, 114) detected H_2O masers in 9 of the 24 regions surveyed around GGD objects, although it is yet to be determined if most of the GGD objects are HH nebulae.

In only one instance (HH 7–11) has an H_2O maser been found to be coincident with a suggested IR source responsible for producing HH

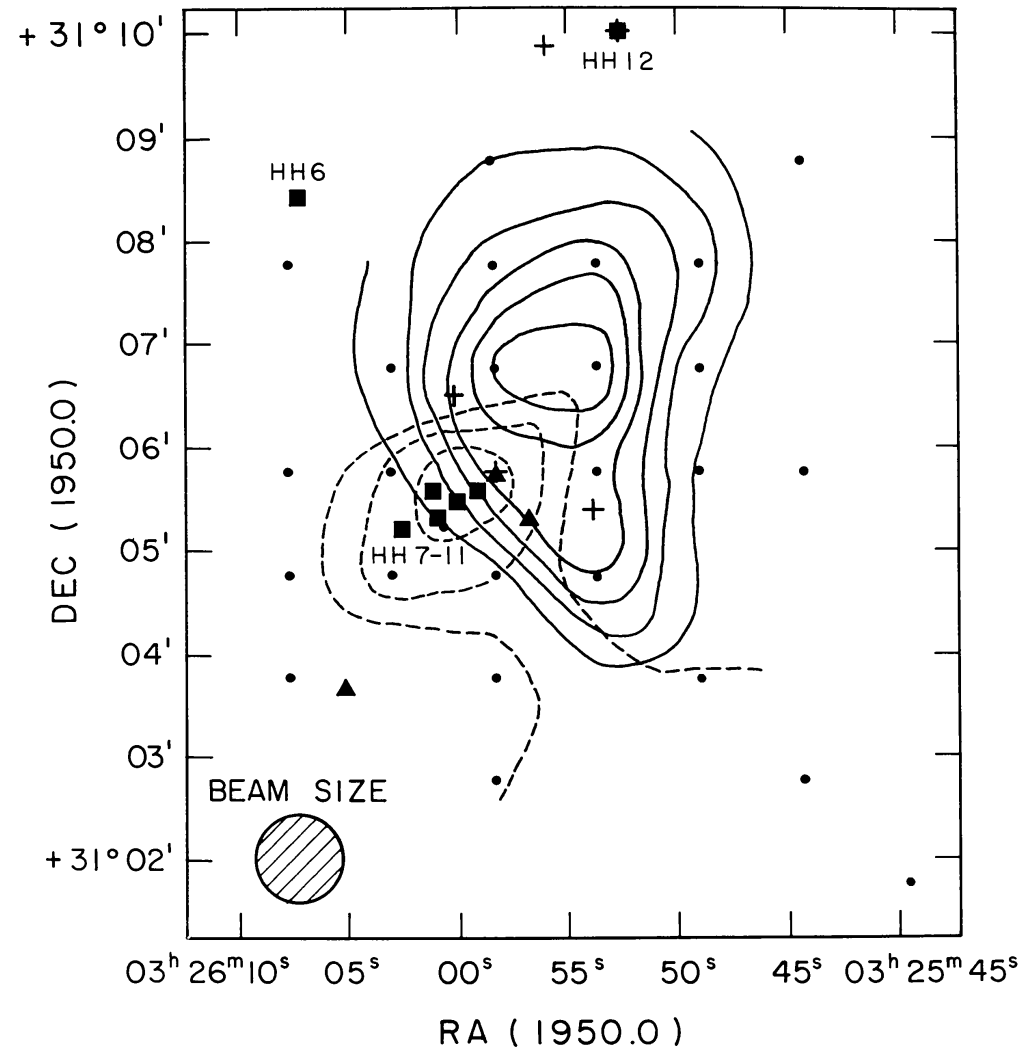

Figure 7 The bipolar CO flow associated with the HH 7–11 IR source. The IR source (+) is coincident with a maser source (*triangle*) and is located about 15″ NW of the linear chain of HH objects that lie in the blueshifted CO lobe [from Snell & Edwards (128) and kindly provided by the authors].

objects. In this case, the interferometric measurements of Haschick et al. (69) suggest a very compact emitting region ($< 7 \times 10^{13}$ cm diameter), which is not entirely consistent with emission from an extended circumstellar shell. Evidently, for H_2O maser emission to occur requires molecular densities of 10^7–10^{10} cm^{-3} and temperatures of 500–1000 K over regions of at least 10–100 AU in extent with relatively low velocity dispersion. It has been suggested that the masing cloud is an isolated fragment (69), possibly related to the "interstellar bullet" theory for the origin of HH objects advanced by Norman & Silk (102) that is discussed in Section 4. Finally, it should be noted that OH emission has been detected from the vicinities of several HH candidates (mostly GGD objects) in the studies of Rodríguez et al. (114), Pashchenko & Rudnitskij (106), and Norris (103).

3.4.4 RADIO CONTINUUM OBSERVATIONS Attempts to detect HH 1 and HH 7–11 at 3.66 GHz were reported by Kandalyan & Sanamyan (84), and upper limits of 20 mJy and 80 mJy, respectively, were found. If it is assumed that HH 1 can be represented by a spherical H II region 0.004 pc in radius with $T_e \sim 10^4$ K and $N_e \sim 3 \times 10^4$ cm^{-3}, 100 mJy should be observable. Using the VLA at 1.5 GHz, B. Balick (private communication) has set upper limits of around 1 mJy for both HH 1 and HH 2. These observations are consistent with the optical observations, which suggest a filling factor of about 0.003 for HH 1 (123), thus predicting a radio flux of about 0.3 mJy. The filling factor strongly supports shock-wave interpretations in which only a thin layer of gas is excited, as opposed to a larger volume which would occur in an H II region. Cohen et al. (37) have recently reported 4.885-GHz observations of T Tau and L 1551 IRS 5, both believed to be exciting stars for HH objects. The two sources yielded 5.8 mJy and 3.5 mJy, respectively, from a region no greater than 0.5 arcsec in diameter. These measurements are interpreted in terms of mass loss from the central stars.

4. THEORETICAL MODELS

The theoretical work on HH objects can be divided into two categories, one dealing with the question of the excitation mechanism for the nebulae and the other with the broader scenario of the physical origin of the objects. A history of proposed excitation mechanisms was summarized in Section 2, and it is now generally believed that dissipation of energy in shock waves is responsible for the HH nebula. In the following subsections we summarize the salient shock-wave calculations, which have been aimed at synthesizing the spectra of HH objects, and the hypotheses that have been advanced about the origin of the objects.

4.1 *Shock-Wave Calculations*

The first attempts to model the optical spectra of HH objects were made by Raymond (108, 109) and Dopita (45) with the use of steady-flow, plane-parallel shock-wave calculations. Approximations to the spectra of HH 1 and HH 2 were obtained with preshock densities of about 300 cm^{-3}, shock velocities of 70–100 km s^{-1}, and solar abundances. In general, the best fits were obtained with low preshock fractional ionizations. A significant revision of Dopita's code incorporating charge-exchange processes and updated atomic data was used by Dopita et al. (48) to synthesize the blue-UV 2q continua and the emission-line intensities of low-excitation HH objects. It was found that only low-velocity ($\lesssim 40$ km s^{-1}), time-truncated shocks (achieved effectively by sawing off part of the recombination zone) propagating in largely neutral atomic material were capable of reproducing the correct relative intensities of emission lines and continuum. Although the shock-wave models of Shull & McKee (126) were geared toward interstellar conditions, they demonstrated that the UV precursor is insignificant at shock velocities used in the HH models; hence, the preshock gas may well be largely neutral.

Owing to the simplifying assumptions made in these shock-wave computations, it is unlikely that they reflect an accurate picture of the true state of HH objects. For example, the clumpy morphology of HH nebulae suggests the presence of nonplanar shocks, or shocks with irregular obliquity. This could lead to large differences in the postshock temperature-density regime as a function of position along the irregular shock front. Also, in the studies cited above no molecular components were included in the preshock gas. Although molecular shock-wave calculations have been carried out by Chernoff et al. (34, and references therein) for objects such as the BN-KL source in Orion, models with density and velocity conditions appropriate for the HH nebulae have not been reported.

4.2 *Hypotheses on the Origin of HH Objects*

A number of scenarios involving the shock-wave production of HH objects have been proposed. Böhm (11) considered the effects of a spherical shock propagating outward through a small cloudlet, showing that the variability of HH nebulae could be explained on this basis. This model requires a source of energy interior to each HH condensation, presumably of a protostellar nature. However, the occurrences of HH alignments with IR sources, HH proper motions, and anisotropic gas flows from the IR sources strongly suggest that HH nebulae are excited extrinsically by young stars.

In a detailed spectroscopic study of HH 1 and HH 2, Schwartz (123) proposed a model wherein a supersonic stellar wind encounters dense

cloudlets in the ambient medium. The stellar wind creates a luminous bow shock around the front side of the cloudlet, which is identified with the HH nebula, and a secondary shock is propagated into the cloudlet with velocity $V = V_w/[1+(n_c/n_w)^{1/2}]$, where V_w is the stellar wind velocity with respect to the cloudlet and n_c and n_w are the cloudlet and wind densities, respectively. It was argued that many of the spectroscopic features of HH nebulae could be produced in such a nonplanar bow shock. In the model, high radial velocities are achieved by acceleration of the cloudlet by the wind. Since the shock velocity (which determines the excitation state of the gas) is the relative velocity between the cloudlet and the stellar wind, the model predicts that the highest velocity objects should possess the lowest excitation spectra, a feature subsequently observed by Schwartz & Dopita (125). Moreover, prebow shock conditions ($V_w \sim 100$ km s^{-1}, $r_w \sim 300$ cm^{-3}) capable of producing the correct optical spectrum will generate a cloudlet shock of about 15 km s^{-1} for a cloudlet density of $n_e \sim 10^4$. If the cloudlet is composed mainly of H_2, this could well represent the source of H_2 IR emission observed by Elias (52). In this hypothesis, light variations would result from episodic changes in the density and/or velocity of the stellar-wind flow. In order to provide enough kinetic energy in a sufficiently small solid angle to excite the nebulae, Schwartz found that mass-loss rates in the range 10^{-6} to 10^{-5} $M_\odot$ yr^{-1} were required *for an isotropic wind.* Recent observations indicating that the flows are highly channeled have obviated the need for such large mass-loss rates, and have suggested that channeled flows of 10^{-8} to 10^{-7} $M_\odot$ yr^{-1} (typical of T Tauri stars) could sustain the HH nebulae. The most serious problem with the stellar-wind-shocked cloudlet model is the problem of momentum transfer from the wind to the cloudlet. Hydrodynamic calculations by Sandford & Whitaker (115) indicate that little acceleration of the cloudlet may be expected. Moreover, the shock-wave structure is complex and may form on the lee side of the cloudlet (115).

The "interstellar bullet" model of Norman & Silk (102) supposes that a pre–T Tauri star develops strong radiation pressure or an intense wind that interacts with infalling natal material. A Rayleigh-Taylor instability at the interface of the two flows produces infalling clumps, which are maintained at high density by the ram pressure of the wind. Eventually, the clumps are swept outward by the wind. While maintained in a dense phase and heated by turbulence from a Kelvin-Helmholtz instability, the clumps are sources of H_2O maser emission. Eventually, the clumps emerge beyond the wind-cloud interface, plowing supersonically into the ambient medium. The resulting shock waves from the shocked ambient medium are identified with the HH nebulae, and the shock geometry and dynamics would have many similarities to the shocked-cloudlet model of Schwartz. The basic

difference is that the Norman-Silk model would shock ambient gas on the side of the clump opposite the star, whereas Schwartz's model involves a shocked stellar wind on the starward side of the cloudlet. The Norman-Silk model might account well for the observations of L 1551 IRS 5 and its associated maser, along with the presence of HH 7–11. One difficulty arises in that high radial velocities of HH cloudlets should be correlated with high-excitation nebulae in the Norman-Silk model. In fact, HH 11 exhibits a very-low-excitation spectrum, but a large radial velocity (-150 km s^{-1}). Another difficulty arises in the identification of the exciting star with a pre–T Tauri stage of evolution. At least five visible, rather normal T Tauri stars (T Tau, HL Tau, AS 353A, RU Lup, and the C-S star) are now known to be associated with HH nebulae, and it is unlikely that these stars have only recently emerged from protostellar cocoons on the timescale (100–1000 yr) consistent with the dynamical lifetime of HH objects.

A model involving a focused stellar wind was proposed by Cantó & Rodríguez (32) [see also Cantó (28, 29), Cantó et al. (31), and Barral & Cantó (4)]. The interaction of an isotropic stellar wind with a surrounding cloud with a pressure gradient was analyzed. A typical scenario might be that of a T Tauri star embedded in the outer parts of a molecular cloud with decreasing cloud density outward. The steady-state solution results in an egg-shaped cavity distended toward the cloud boundary, with the stellar-wind flow strongly refracted at the wind-cloud interface. The refracted, annular stream converges to the distant outer tip of the ovoid (near the outer boundary of the cloud) and produces a shock at that point, which is identified with an HH nebula. Barral & Cantó (4) extended this to a study of the flow of an isotropic wind into a large "interstellar disk" around a star, showing that a bipolar flow would result. These models have the distinct advantage of reducing the total stellar-wind energy requirements by the focusing mechanisms. However, the resultant dynamics of the shocked material are not clear, and the model probably cannot produce high-velocity HH objects (80).

With the growing evidence for well-collimated, bipolar flows associated with young stellar objects in molecular clouds, Königl (88) has analyzed in detail the generation of bipolar jets from the expansion of a stellar wind in a circumstellar disk with an inhomogeneous density distribution. For disk density distributions expected in protostellar environments, Königl shows that the expanding stellar-wind bubble may become unstable to the formation of de Laval nozzles, which channel the flow into oppositely directed, supersonic jets. It is speculated that the HH nebulae result when clumps of matter are accelerated by the jet. As in the shocked-cloudlet scenario, however, it is not clear whether such acceleration is hydrodynamically possible with a stellar wind. If the cloudlets remain coherent in such a

flow, it is possible that they are compressed into pancake-like configurations during the acceleration process. Like the Norman & Silk model, Königl considers the mechanism in terms of "protostellar" activity, and his model may not easily account for the HH objects associated with visible T Tauri stars.

While most of the aforementioned models require the presence of a steady or quasi-steady stellar-wind flow, evidence is mounting that the HH objects may be the result of eruptive events in T Tauri stars. Mundt & Hartmann (100) have recently carried out high-dispersion spectroscopic observations of the C-S star between HH 1 and HH 2, discovering that the star now appears rather quiescent (weak T Tauri activity) with no indication of large-scale, continuous mass loss. At the same time, Böhm & Böhm-Vitense (14) have found a substantial diffuse source of UV radiation with a luminosity of at least 340 $L_\odot$ apparently associated with the C-S star. Since IR and optical observations indicate a present luminosity for the star that is about 10 times less than this, an eruptive event must have occurred at some time in the past to deposit this energy into the surrounding environment, and incidentally to create the HH objects, which themselves possess radiative luminosities of roughly 1 $L_\odot$ and kinetic energies of perhaps 10^{42} ergs.

The most likely eruptive event known to be associated with T Tauri stars is the FU Orionis phenomenon, in which a star may undergo a hundredfold increase of luminosity on a timescale of months, fading gradually to its original luminosity on a timescale of many decades. Dopita (45, 46) earlier suggested that some HH objects might result from the breakup of cocoons around either B stars or FU Ori stars, and Gyul'budagyan (59) had also suggested a connection between HH objects and FU Ori stars. Known FU Ori stars have reached luminosities of $\sim 10^3$ $L_\odot$ before slowly fading, and they exhibit evidence of rapidly ejected material (79). Moreover, Herbig (79) estimates a repetitive timescale of $\sim 10^4$ yr for such eruptions in an average T Tauri star, a rate that is roughly in accord with the number of HH objects if their radiative lifetimes are of the order of 10^3 yr or less.

One of the most persuasive theoretical treatments of the FU Ori phenomenon has been given by Larson (91), who shows that rapid stellar rotation may lead to a barlike instability in a star, which results in the deposition of large amounts of energy into the outer stellar layers and leads to the eruption. It would be of great interest to follow the consequences of such an eruption in the presence of a circumstellar disk to see if bipolar jets might emerge. Of the several FU Ori stars that have been observed to erupt within recent history, none are presently associated with HH objects. This may be caused by the fact that previous eruptions have evacuated rather large cavities around the stars, and material from the more recent eruptions

has not yet reached the cavity boundaries, where it might interact with the ambient medium to produce shock-excited nebulae. In this regard it would be important to continue monitoring known FU Ori stars and their environments for such a phenomenon.

5. CONCLUSION

Our present knowledge of HH objects has benefited from recent observational studies spanning a wide spectral range. In combination with theoretical modeling, these studies suggest the following conclusions:

1. The luminosities of HH nebulae derive largely from shock-wave excitation with shock velocities in the range 40–100 km s^{-1}, and preshock densities of 100–300 cm^{-3} with low fractional ionization.
2. A few HH objects exhibit red continuum that is polarized, indicating that dust coterminous with the emission nebula is reflecting light from the exciting star. Probably all HH objects possess a blue-UV continuum, which may be due mainly to in situ two-photon emission enhanced by collisional excitation.
3. In a number of cases, linear alignments of HH nebulae with embedded IR sources and proper motions of the nebulae indicate that the nebulae are produced by anisotropic stellar mass loss.
4. Bipolarlike molecular flows aligned upon HH objects and centered upon the exciting IR sources in several cases provide further evidence of focused mass loss.
5. The association of five T Tauri stars with HH objects, and the IR energy distributions and luminosities of embedded sources associated with HH objects, suggest that the exciting stars are young, relatively low mass stars.
6. Luminosity variations and total energies (radiative plus kinetic) of HH objects, combined with the present quiescent states of their exciting stars, indicate that at least some objects may result from eruptive events in young stars.

A number of projects could further illuminate the nature of HH objects and their exciting stars. High-resolution UV spectra with improved signal-to-noise ratios will probably be required to determine the detailed shape of the continuum. Monochromatic imagery of HH nebulae obtained at high spatial resolution in emission lines covering a wide range of excitation could in principle reveal shock-wave stratification. Whereas these two projects will probably require use of the Space Telescope, important ground-based investigations remain to be done.

First, spectrophotometric study of variable HH nebulae carried out

frequently over a period of years with the same equipment and reduction procedures could yield important information on the time-dependent character of the shock-wave structure. Second, combined proper motion and radial velocity data can yield space motions of HH objects. In cases where bipolar ejection is indicated (e.g. HH 46/47, H 1/2), this could be used to infer the orientation of the axis of ejection (the rotation axis?) of the star. Third, more detailed IR and radio measurements of the exciting stars and their molecular gas flows will be required to obtain a better picture of the total energies associated with the HH phenomenon. On the theoretical side, investigation of nonsteady, nonplanar shocks may be required to understand the HH spectra in detail. Finally, mechanisms that can produce anisotropic mass loss—possibly in eruptive events—should be explored for T Tauri stars.

ACKNOWLEDGMENTS

I would like to thank G. H. Herbig, R. L. Snell, and B. Bok for providing illustrations for this review. This work was supported in part by NSF grant AST 8201430.

Literature Cited

1. Adams, M. T., Strom, K. M., Strom, S. E. 1979. *Ap. J. Lett.* 230:L183
2. Ambartsumian, V. A. 1954. *Commun. Burakan Obs. No. 13*
3. Bally, J., Lada, C. J. 1983. *Ap. J.* 265:824
4. Barral, J. F., Cantó, J. 1981. *Rev. Mex. Astron. Astrofis.* 5:101
5. Beckwith, S., Gatley, I., Matthews, K., Neugebauer, G. 1978. *Ap. J. Lett.* 223:L41
6. Beichman, C., Harris, S. 1981. *Ap. J.* 245:589
7. Böhm, K.-H. 1956. *Ap. J.* 123:379
8. Böhm, K.-H. 1975. In *Problems in Stellar Atmospheres and Envelopes*, ed. E. Baschek, W. H. Kegel, G. Traving, p. 205. Berlin: Springer
9. Böhm, K.-H. 1977. In *Proc. IAU Colloq. No. 42, The Interaction of Variable Stars with their Environment*, ed. R. Kippenhahn, J. Rahe, W. Strohmeier, p. 3
10. Böhm, K.-H. 1978. In *Protostars and Planets: Studies of Star Formation and the Origin of the Solar System*, ed. T. Gehrels, p. 632. Tucson: Univ. Ariz. Press
11. Böhm, K.-H. 1978. *Astron. Astrophys.* 64:115
12. Böhm, K.-H. 1979. In *Problems of Physics and Evolution of the Universe*, ed. L. V. Mirzoyan, p. 121. Erevan: Publ. House Armenian Acad. Sci.
13. Böhm, K.-H., Böhm-Vitense, E., Brugel, E. W. 1981. *Ap. J. Lett.* 245:L113
14. Böhm, K.-H., Böhm-Vitense, E. 1982. *Ap. J. Lett.* 263:L35
15. Böhm, K.-H., Brugel, E. W. 1979. *Astron. Astrophys.* 74:297
16. Böhm, K.-H., Brugel, E. W., Mannery, E. 1980. *Ap. J. Lett.* 235:L137
17. Böhm, K.-H., Perry, J. F., Schwartz, R. D. 1973. *Ap. J.* 179:149
18. Böhm, K.-H., Schwartz, R. D., Siegmund, W. A. 1974. *Ap. J.* 193:353
19. Böhm, K.-H., Siegmund, W. A., Schwartz, R. D. 1976. *Ap. J.* 203:399
20. Böhm-Vitense, E., Böhm, K.-H., Cardelli, J. A., Nemec, J. M. 1982. *Ap. J.* 262:224
21. Brown, A., Jordan, C., Millar, T. J., Gondhalekar, P., Wilson, R. 1981. *Nature* 290:34
22. Brugel, E. W., Böhm, K.-H., Mannery, E. 1981. *Ap. J.* 243:874
23. Brugel, E. W., Böhm, K.-H., Mannery, E. 1981. *Ap. J. Suppl.* 47:117
24. Brugel, E. W., Shull, J. M., Seab, C. G. 1982. *Ap. J. Lett.* 262:L35
25. Burnham, S. W. 1890. *MNRAS* 51:94

26. Burnham, S. W. 1894. *Publ. Lick Obs.* 2:175
27. Calvet, N., Cantó, J., Rodríguez, L. F. 1983. *Ap. J.* In press
28. Cantó, J. 1979. PhD thesis. Univ. Manchester
29. Cantó, J. 1980. *Astron. Astrophys.* 86:327
30. Cantó, J. 1981. In *Investigating the Universe*, ed. F. D. Kahn, p. 95. Dordrecht: Reidel
31. Cantó, J., Goudis, C., Johnson, P. G., Meaburn, J. 1980. *Astron. Astrophys.* 85:128
32. Cantó, J., Rodríguez, L. F. 1980. *Ap. J.* 239:982
33. Cantó, J., Rodríguez, L. F., Barral, J. F., Carral, P. 1981. *Ap. J.* 244:102
34. Chernoff, D. F., Hollenbach, D. J., McKee, C. F. 1982. *Ap. J. Lett.* 259: L97
35. Cohen, M. 1980. *Ap. J.* 85:29
36. Cohen, M. 1980. *MNRAS* 191:499
37. Cohen, M., Bieging, J. H., Schwartz, P. R. 1982. *Ap. J.* 253:707
38. Cohen, M., Schmidt, G. D. 1981. *Astron. J.* 86:1228
39. Cohen, M., Schwartz, R. D. 1979. *Ap. J. Lett.* 233:L77
40. Cohen, M., Schwartz, R. D. 1980. *MNRAS* 191:165
41. Cohen, M., Schwartz, R. D. 1983. *Ap. J.* 265:877
42. Cudworth, K. M., Herbig, G. H. 1979. *Astron. J.* 84:548
43. Dickinson, D. F., Kojoian, G., Strom, S. E. 1974. *Ap. J. Lett.* 194:L93
44. Dopita, M. A. 1978. *Astron. Astrophys.* 63:237
45. Dopita, M. A. 1978. *Ap. J. Suppl.* 37:117
46. Dopita, M. A. 1978. In *Planetary Nebulae: Observations and Theory*, ed. Y. Terzian, p. 324. Dordrecht: Reidel
47. Dopita, M. A. 1981. In *Investigating the Universe*, ed. F. D. Kahn, p. 29. Dordrecht: Reidel
48. Dopita, M. A., Binette, L., Schwartz, R. D. 1982. *Ap. J.* 261:183
49. Dopita, M. A., Schwartz, R. D., Evans, I. 1982. *Ap. J. Lett.* 263:L73
50. Edwards, S., Snell, R. L. 1982. *Ap. J.* 261:151
51. Elias, J. H. 1978. *Ap. J.* 224:857
52. Elias, J. H. 1980. *Ap. J.* 241:728
53. Fischer, J., Righini-Cohen, G., Simon, M. 1980. *Ap. J. Lett.* 238:L155
54. Fridlund, C. V. M., Nordh, H. L., van Duinen, R. J., Aalders, J. W. G., Sargent, A. I. 1980. *Astron. Astrophys.* 91:L1
55. Gahm, G. F. 1980. *Ap. J. Lett.* 242:L163
56. Gull, T. R., Goad, L., Chiu, H.-Y., Maran, S. P., Hobbs, P. W. 1973. *Publ. Astron. Soc. Pac.* 85:526
57. Gurzadyan, G. A. 1974. *Astron. Astrophys.* 33:307
58. Gurzadyan, G. A. 1975. *Astrofizika* 11:531
59. Gyul'budagyan, A. L. 1975. *Astrofizika* 11:511
60. Gyul'budagyan, A. L. 1977. *Dokl. Akad. Nauk Arm. SSR* 65:35
61. Gyul'budagyan, A. L. 1980. In *Flare Stars, FUORS, and H-H Objects*, ed. L. V. Mirzoyan, p. 327. Yerevan: Publ. House Acad. Sci. Arm. SSR
62. Gyulbudaghian, A. L., Glushkov, Yu. I., Denisyuk, E. K. 1978. *Ap. J. Lett.* 224:L137
63. Haro, G. 1950. Private communication of May 31 to Drs. H. Shapely and R. Minkowski
64. Haro, G. 1952. *Ap. J.* 115:572
64a. Haro, G. 1953. *Ap. J.* 117:73
65. Haro, G., Iriarte, B., Chavira, E. 1953. *Bol. Obs. Tonantzintla Tacubaya* 8:3
66. Haro, G., Minkowski, R. 1960. *Astron. J.* 65:490
67. Harvey, P. M., Leverault, R., Cohen, M. 1981. *Bull. Am. Astron. Soc.* 13:541
68. Harvey, P. M., Wilking, B., Cohen, M. 1981. In *Proc. Henry Draper Symp., Dec., New York Univ.*
69. Haschick, A. D., Moran, J. M., Rodríguez, L. F., Burke, B. F., Greenfield, P., Garcia-Baretto, J. A. 1980. *Ap. J.* 237:26
70. Haschick, A. D., Moran, J. M., Rodríguez, L. F., Ho, P. T. P. 1982. *Ap. J.* 265:281
71. Herbig, G. H. 1950. *Ap. J.* 111:11
72. Herbig, G. H. 1951. *Ap. J.* 113:697
73. Herbig, G. H. 1952. *J. R. Astron. Soc. Can.* 46:222
74. Herbig, G. H. 1957. In *IAU Symp. No. 3*, ed. G. H. Herbig, p. 3. Cambridge Univ. Press
75. Herbig, G. H. 1969. In *Non-Periodic Phenomena in Variable Stars*, ed. L. Detre, p. 75. Dordrecht: Reidel
76. Herbig, G. H. 1970. In *Spectroscopic Astrophysics*, ed. G. H. Herbig, p. 237. Berkeley: Univ. Calif. Press
77. Herbig, G. H. 1973. *Commun. 27 IAU Inf. Bull. Var. Stars No. 832*
78. Herbig, G. H. 1974. *Lick Obs. Bull. No. 658*
79. Herbig, G. H. 1977. *Ap. J.* 217:693
80. Herbig, G. H., Jones, B. F. 1981. *Astron. J.* 86:1232
81. Ho, P. T. P., Barrett, A. H. 1980. *Ap. J.* 237:38
82. Johnston, K. J., Knowles, S. H., Sullivan, W. T. 1971. *Ap. J. Lett.* 167:L93

83. Jones, B. F., Herbig, G. H. 1982. *Astron. J.* 87:1223
84. Kandalyan, R. A., Sanamyan, V. A. 1979. *Astrofizika* 15:705
85. King, D. J., Scarrott, S. M. 1981. *Observatory* 101:197
86. Knapp, G. R., Kuiper, T. B. H., Knapp, S. L., Brown, R. L. 1976. *Ap. J.* 206:443
87. Knapp, G. R., Morris, M. 1976. *Ap. J.* 206:713
88. Königl, A. 1982. *Ap. J.* 261:115
89. Kutner, M. L., Leung, C. M., Machnik, D. E., Mead, K. N. 1982. *Ap. J. Lett.* 259:L35
90. Lada, C. J., Gottlieb, C. M., Litvak, M. M., Lilley, A. E. 1974. *Ap. J.* 194:609
91. Larson, R. B. 1980. *MNRAS* 190:321
92. Lo, K. Y., Burke, B. F., Haschick, A. D. 1975. *Ap. J.* 202:81
93. Lo, K. Y., Morris, M., Moran, J. M., Haschick, A. D. 1976. *Ap. J. Lett.* 204:L21
94. Loren, R. B. 1976. *Ap. J.* 209:466
95. Loren, R. B., Evans, N. J. III, Knapp, G. R. 1979. *Ap. J.* 234:932
95a. Luyten, W. J. 1963. *Harvard Ann.* Card No. 1589
95b. Luyten, W. J. 1971. *The Hyades.* Minneapolis: Univ. Minn. Press
96. MacDonald, G. H., Little, L. T., Brown, A. T., Riley, P. W., Matheson, D. N., Felli, M. 1981. *MNRAS* 195:387
97. Magnan, C., Schatzman, E. 1965. *C. R. Acad. Sci. Paris* 260:6289
98. Moorwood, A. F. M., Salinari, P. 1981. *Astron. Astrophys.* 94:299
99. Münch, G. 1977. *Ap. J. Lett.* 212:L77
100. Mundt, R., Hartmann, L. 1982. Preprint
101. Mundt, R., Stocke, J., Stockman, H. S. 1982. *Ap. J. Lett.* 265:L71
102. Norman, C. A., Silk, J. 1979. *Ap. J.* 228:197
103. Norris, R. P. 1980. *MNRAS* 193:39p
104. Ortolani, S., D'Odorico, S. 1980. *Astron. Astrophys.* 83:L8
105. Osterbrock, D. E. 1958. *Publ. Astron. Soc. Pac.* 70:399
106. Pashchenko, M. J., Rudnitskij, G. M. 1980. *Astron. Zh.* 57:1204
107. Pravdo, S. H., Marshall, F. E. 1981. *Ap. J.* 248:591
108. Raymond, J. 1976. PhD thesis. Univ. Wis. Madison
109. Raymond, J. 1979. *Ap. J. Suppl.* 39:1
110. Reipurth, B. 1981. *Astron. Astrophys. Suppl.* 44:379
111. Rodríguez, L. F. 1981. *Mercury* 10:34
112. Rodríguez, L. F., Carral, P., Ho, P. T. P., Moran, J. M. 1982. *Ap. J.* 260:635
113. Rodríguez, L. F., Moran, J. M., Dickinson, D. F., Gyulbudaghian, A. L. 1978. *Ap. J.* 226:115
114. Rodríguez, L. F., Moran, J. M., Ho, P. T. P., Gottlieb, E. W. 1980. *Ap. J.* 235:845
114a. Rydgren, A. E., Strom, S. E., Strom, K. M. 1976. *Ap. J. Suppl.* 30:307
115. Sandford, M. T., Whitaker, R. W. 1982. Preprint
116. Schmidt, G. D., Miller, J. S. 1979. *Ap. J. Lett.* 234:L191
117. Schmidt, G. D., Vrba, F. J. 1975. *Ap. J. Lett.* 201:L33
118. Schwartz, R. D. 1974. *Ap. J.* 191:419
119. Schwartz, R. D. 1975. *Ap. J.* 195:631
120. Schwartz, R. D. 1976. *Publ. Astron. Soc. Pac.* 88:159
121. Schwartz, R. D. 1977. *Ap. J. Lett.* 212:L25
122. Schwartz, R. D. 1977. *Ap. J. Suppl.* 35:161
123. Schwartz, R. D. 1978. *Ap. J.* 223:884
124. Schwartz, R. D. 1981. *Ap. J.* 243:197
124a. Schwartz, R. D. 1983. *Ap. J. Lett.* In press
125. Schwartz, R. D., Dopita, M. A. 1980. *Ap. J.* 236:543
126. Shull, J. M., McKee, C. F. 1979. *Ap. J.* 227:131
127. Simon, T., Joyce, R. R. 1983. *Ap. J.* 265:864
128. Snell, R. L., Edwards, S. 1981. *Ap. J.* 251:103
129. Snell, R. L., Edwards, S. 1982. *Ap. J.* 259:668
130. Snell, R. L., Loren, R. B., Plambeck, R. L. 1980. *Ap. J. Lett.* 239:L17
131. Strom, K. M., Strom, S. E., Grasdalen, G. L. 1974. *Ap. J.* 187:83
132. Strom, K. M., Strom, S. E., Kinman, T. D. 1974. *Ap. J. Lett.* 191:L93
133. Strom, K. M., Strom, S. E., Vrba, F. J. 1976. *Astron. J.* 81:308
134. Strom, K. M., Strom, S. E., Vrba, F. J. 1976. *Astron. J.* 81:320
135. Strom, S. E., Grasdalen, G. L., Strom, K. M. 1974. *Ap. J.* 191:111
136. Strom, S. E., Strom, K. M., Grasdalen, G. L. 1975. *Ann. Rev. Astron. Astrophys.* 13:187
137. Strom, S. E., Strom, K. M., Vrba, F. J. 1976. *Astron. J.* 81:314
138. Strom, S. E., Strom, K. M., Vrba, F. J. 1976. *Astron. J.* 81:638
139. Vrba, F. J., Strom, S. E., Strom, K. M. 1975. *Publ. Astron. Soc. Pac.* 87:337
140. Vrba, F. J., Strom, S. E., Strom, K. M. 1976. *Astron. J.* 81:317
141. Whittet, D. C. B., Blades, J. C. 1981. *MNRAS* 191:309